ARTICLE IN PRESS

Materials Today: Proceedings xxx (xxxx) xxx

Contents lists available at ScienceDirect

Materials Today: Proceedings

journal homepage: www.elsevier.com/locate/matpr

Influence of agglomerations on magnetic properties of polymer matrices filled with magnetic nanoparticles

Tomasz Blachowicz [a], Jacek Grzybowski [b], Andrea Ehrmann [c,*]

[a] Institute of Physics – Centre for Science and Education, Silesian University of Technology, 44 100 Gliwice, Poland
[b] Faculty of Automatic Control, Electronics and Computer Science, Silesian University of Technology, 44 100 Gliwice, Poland
[c] Faculty of Engineering and Mathematics, Bielefeld University of Applied Sciences, 33619 Bielefeld, Germany

ARTICLE INFO

Article history:
Available online xxxx

Keywords:
Magnetic nanoparticles
Electrospinning
Magnetite
Nickel-ferrite
Maghemite

ABSTRACT

Magnetic nanoparticles can be embedded in electrospun nanofibers and other polymeric matrices to prepare magnetic composites with defined magnetic and mechanical properties. Metal-oxide nanoparticles, such as magnetite or nickel-ferrite, are of special interest since they do not need a coating to avoid oxidation. Like other nanoparticles, these metal-oxide nanoparticles tend to form agglomerations, in this way modifying the magnetic properties of the composites. After studying this effect for the magnetic elements Co, Fe, Ni as well as permalloy (Py) in a previous study, defining a new method to quantify the nanoparticle distribution in a polymer, here we concentrate on the influence of agglomerations on the magnetic properties of metal-oxide nanoparticles with different diameters in non-magnetic matrices.

1. Introduction

Composites from ferro- or ferrimagnetic nanoparticles embedded in nonmagnetic matrices can be used in a broad range of applications. Potential utilizations are heating, imaging, catalysis or sensors [1–3] as well as spintronics, data storage and neuromorphic computing [4–6]. For all these applications, it is necessary to characterize the nanoparticles as well as the complete composites in terms of their magnetic properties. Such investigations of pure nanoparticles and nanoparticle clusters are thus often reported in the literature [7–9].

The influence of clustering nanoparticles is usually investigated for regular clusters, e.g. two-dimensional lattices with square or hexagonal structure [10–12]. Simulations of magnetic properties become more complicated if three-dimensional lattices are filled with magnetic nanoparticles [13,14]. Most challenging, however, are composites in which magnetic nanoparticles are arbitrarily distributed in a nonmagnetic matrix, especially if the number and volumes of agglomerations are unclear. Such composites have been investigated, e.g., by ferromagnetic resonance [15,16] or common static methods, such as superconducting quantum interference device (SQUID), alternating gradient magnetometer (AGM) or vibrating sample magnetometer (VSM) [17–19].

Simulations of these composites are only scarcely found in the literature. Self-assembled clusters of up to four permalloy (Py) nanoparticles in varying geometries were reported to show different magnetic properties, depending on the structure of this agglomeration [20]. Arrays of regularly distributed round FePt nanoparticle showed a significant influence of the exchange interaction on remanence, coercive field and shape of the simulated hysteresis loops [21]. Nickel nanoparticles, nanoparticle chains and clusters were found to show different magnetic properties [22,23]. For clustered CoPt and FePt nanoparticles with varying diameters, the amount of uniaxial and cubic phases was investigated, while the impact of the nanoparticle distance was not further taken into account [24].

In a previous study of our group, distributed nanoparticles with large distances were compared with agglomerations of different sizes, showing significant differences in the hysteresis loop shapes and coercive fields [25]. Besides, we varied sets of Co, Fe, Ni, and Py nanoparticles of different average diameters between fully agglomerated and fully separated states, showing a strong influence of the distribution especially for cobalt and permalloy [26]. Here, the system developed in [26] was used to investigate mag-

* Corresponding author.
E-mail address: andrea.ehrmann@fh-bielefeld.de (A. Ehrmann).

https://doi.org/10.1016/j.matpr.2022.07.362

netic metal-oxide particles which are often used in electrospun and other nonmagnetic matrices [27–29].

2. Materials and methods

The micromagnetic solver Magpar [30] was used to perform micromagnetic simulations on nanoparticle clusters of magnetic spheres with varying diameters. The materials under examination here were magnetite (Fe_3O_4), nickel-ferrite (Fe_2O_3/NiO), and maghemite (γ-Fe_2O_3). The corresponding parameters are depicted in Table 1.

The cluster formation process is described in detail elsewhere [26]. In brief, a sphere of diameter 540 nm – i.e. an average diameter of electrospun nanofibers – was filled with spheroid nanoparticles with diameters (50 ± 8.3) nm, (75 ± 12.5) nm, and (100 ± 6.7) nm, respectively. Different concentrations were tested, namely 0.3 vol% and 1.75 vol% for an average diameter of 50 nm, 0.9 vol % and 20 vol% for 75 nm mean diameter, and 2.1 vol% and 40 vol % for 100 nm, respectively. As the starting point, full agglomeration is reached by moving all nanoparticles to the middle of the large sphere until they touch. This situation is defined as an expansion ratio of 1. Then, the particles are moved out of the center radially by different factors, based on the original agglomerated distance to the middle of the sphere, up to a factor of 8.99. Depending on the original concentration, the nanoparticles were in some cases positioned outside the original sphere; this method was applied to ensure reaching distances in which interactions between neighboring nanoparticles can be neglected. An example of particles with 100 nm average diameter, completely agglomerated and maximally expanded, for concentrations of 2.1 vol% and 40 vol% is given in Fig. 1; more situations are depicted in Ref. [26].

In all simulations, the hysteresis loops were simulated orienting the external magnetic field along the x-axis, which is identical to the easy anisotropy axes of Fe_3O_4 and Fe_2O_3/NiO and to the hard axis of γ-Fe_2O_3.

3. Results and discussion

Fig. 2 shows exemplary hysteresis loops of nickel-ferrite nanoparticle systems, using an average diameter of 75 nm, both corresponding concentrations of 0.9% and 20%, and full agglomeration (expansion = 1) as well as maximum distribution (expansion = 8.99). On the one hand, larger expansions lead to larger coercive fields and more square-like hysteresis loops, as it can be expected for measurements along an easy axis and was also visible for simulations of Co [26]. On the other hand, for the smaller concentration (Fig. 2a), strong oscillations of the magnetization are visible, which can be attributed to the small damping factor in the simulation (α = 0.1, as usual for nickel-ferrite and some other magnetic metal oxides) [31–33]. Interestingly, besides the reduced oscillations for a higher material concentration (Fig. 2b), no large differences are visible between concentrations of 0.9% and 20%.

Table 1
Model parameters of simulated materials.

Parameter	Fe_3O_4	Fe_2O_3/NiO	γ-Fe_2O_3
anisotropy constants	$K_1 = -1.1 \times 10^4$	$K_1 = -6.9 \times 10^3$ J/m^3	$K_1 = 4.0 \times 10^4$ J/m^3
exchange constant A	1.0×10^{-11} J/m	1.2×10^{-11} J/m	1.32×10^{-11} J/m
magnetic polarization at saturation J_S	0.6 T	0.339 T	0.4 T
Gilbert damping constant α	0.1	0.1	0.1

Next, maghemite nanoparticle systems are investigated for an average diameter of 75 nm and maximum and minimum expansion rates (Fig. 3). These curves have a completely different shape, corresponding to the different magnetic properties and the measurement along a hard axis, opposite to nickel-ferrite (cf. Table 1), slightly similar to previous simulations of Fe systems [26]. For both concentrations, the coercive fields are very small, and the hysteresis curves look like typical hard axis loops. With increasing expansion, the coercive fields become smaller. No oscillations are visible, independent of expansion or concentration (α = 0.1).

Finally, Fig. 4 depicts hysteresis loops of magnetite, simulated for the same averaged diameter of 75 nm and maximum as well as minimum expansion rates and concentrations, respectively. Magnetite shows intermediate magnetic properties between those of nickel-ferrite and maghemite, corresponding to its anisotropy constant which is between the other values. While the expanded systems result in a similar shape of the hysteresis loop for both concentrations, the agglomerated states differ, with a double-hysteresis loop for the lower concentration. Indeed, this system (75 nm, concentration 0.9%) consists of only 3 nano-spheres [26], explaining this effect which is else typically reported from thin-film systems containing two magnetic layers with different coercive fields and thus switching subsequently. For the higher concentration, no such effect is visible.

In the next step, the influence of concentrations, expansion rates and average nanoparticle diameters on the coercive fields is examined. Fig. 5 depicts the results of these evaluations.

For nickel-ferrite (Fig. 5a), a general tendency is visible towards firstly decreasing coercive fields with increasing expansion ratio, followed by a stronger increase of the coercive field for higher expansion ratios. The minimum coercive fields can be found at expansion ratios around 1.5–3.5, depending on the average nanoparticle diameter and the material concentration. Most importantly, there is no saturation visible at large expansion ratios, opposite to all other materials investigated previously [26]. Apparently, in case of nickel-ferrite, even larger distances between the single nanoparticles have to be investigated in the future.

This is different for maghemite (Fig. 5b). Here, saturation is reached for expansion ratio above approx. 5. The general trend of the curves is in all cases identical, with 100 nm/40% concentration showing the smallest coercive fields for small expansion ratios. This clear decrease of the coercive fields with increasing expansion is contrary to the previous findings, where Ni and Fe showed a relatively small influence of the expansion ratio on the coercive field, while coercive fields increase with increasing expansion ratio for Co and Py [26]. These findings underline the importance of modeling distributed nanoparticles in nonmagnetic matrices for each magnetic material again, since neither elemental magnets [26] nor metal oxide magnets, as investigated here by the examples of nickel-ferrite and maghemite, show a common trend for all materials.

Finally, magnetite shows a varying expansion ratio-dependence for different systems. The systems containing nanoparticles of average diameter 50 nm behave similar to those prepared from nickel-ferrite, with minimum coercive fields for an intermediate expansion ratio. Both systems with average diameters of 75 nm show only a very small minimum, followed by a strong increase in the coercive field. For the systems with 100 nm average diameter, finally, the concentration also influences the coercive fields. These results show the strong influence of the nanoparticle distribution in a nonmagnetic matrix, especially for magnetite which is often used as a magnetic filler in electrospun nanofiber or other polymeric matrices, and suggest using small nanoparticles in case of magnetite to reduce this effects which may make measurements irreproducible [25].

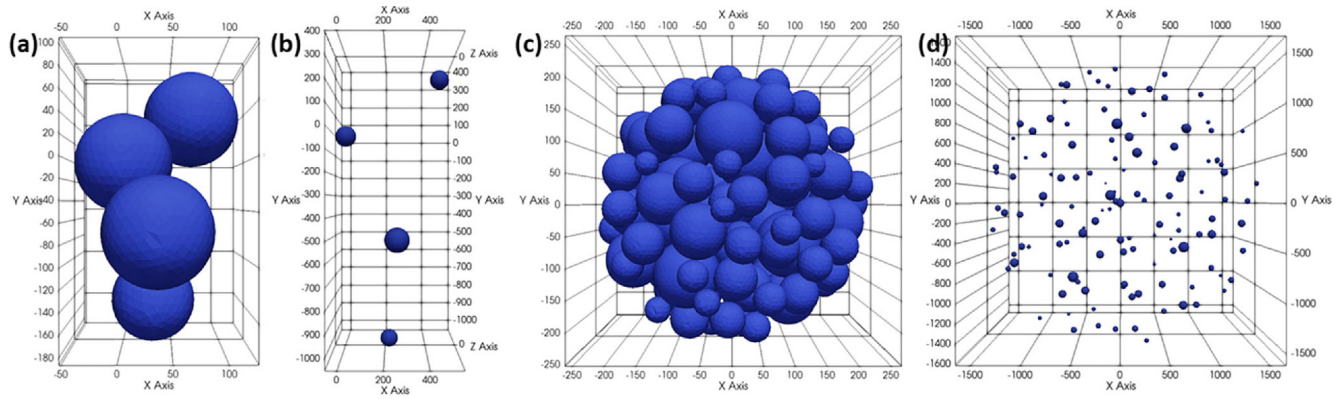

Fig. 1. Systems with average particle diameters of 100 nm: concentration 2.1 vol% (a) fully agglomerated; (b) maximally expanded; concentration 40 vol% (c) fully agglomerated; (d) maximally expanded.

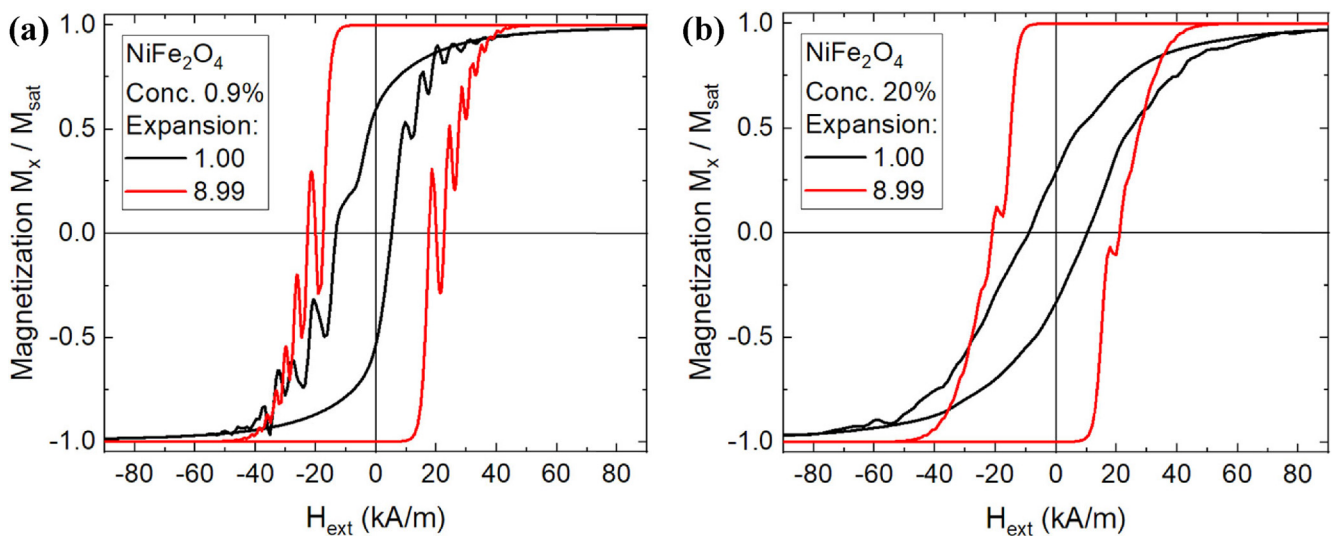

Fig. 2. Nickel-ferrite nanoparticles of average diameter 75 nm with different expansion rates and concentrations of (a) 0.9%; (b) 20%, related to the original sphere size.

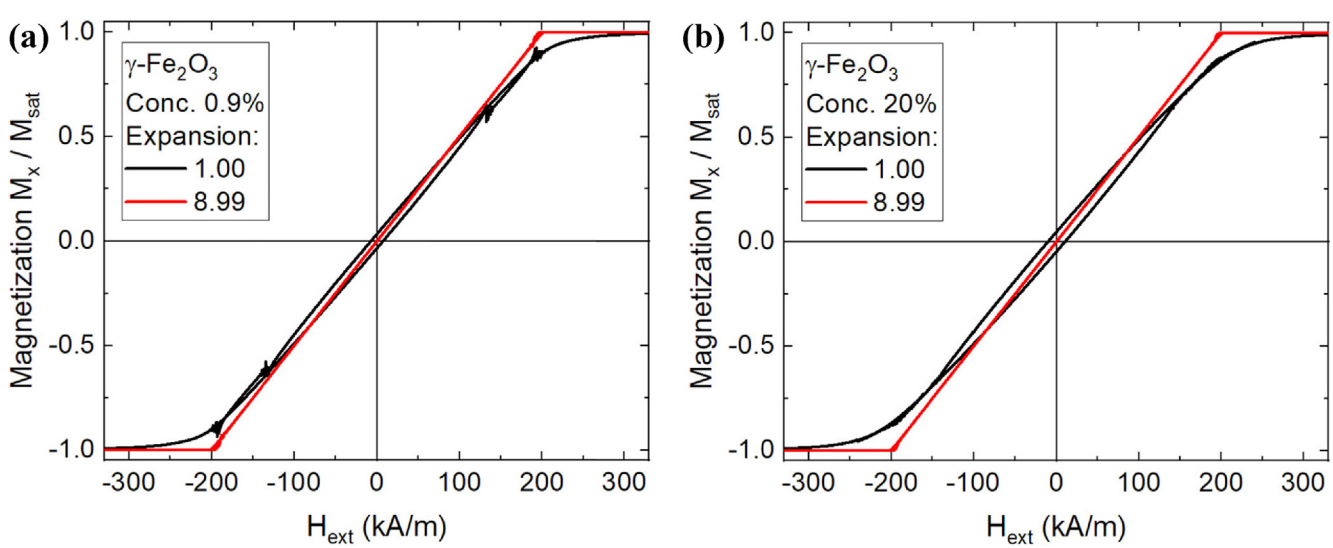

Fig. 3. Maghemite nanoparticles of average diameter 75 nm with different expansion rates and concentrations of (a) 0.9%; (b) 20%, related to the original sphere size.

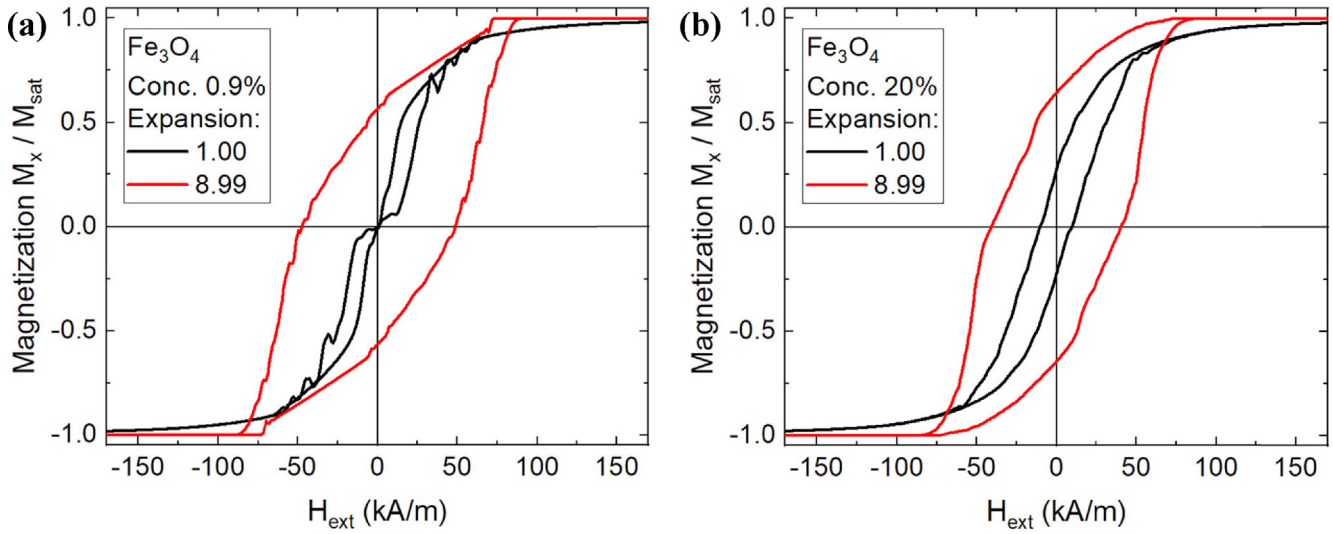

Fig. 4. Magnetite nanoparticles of average diameter 75 nm with different expansion rates and concentrations of (a) 0.9%; (b) 20%, related to the original sphere size.

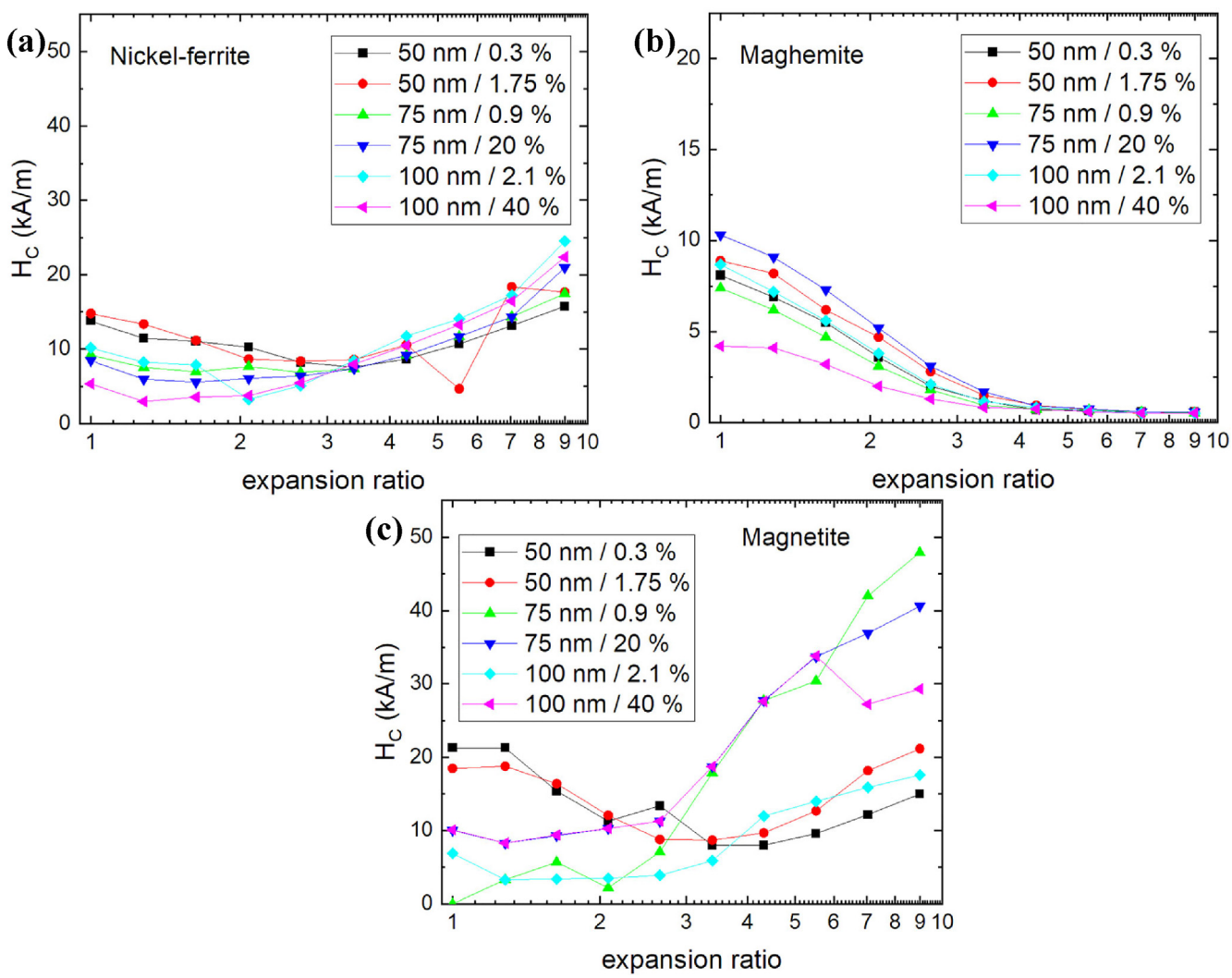

Fig. 5. Coercive fields H_C, dependent on average nanoparticle diameters, concentrations and expansion ratios, for (a) nickel-ferrite; (b) maghemite, (c) magnetite nanoparticles.

4. Conclusion

A series of simulations of the magnetic metal-oxides nickel-ferrite and maghemite was performed by the micromagnetic solver Magpar, investigating nanoparticles of different diameters distributed in a nonmagnetic matrix. The results for both materials differ strongly. While nickel-ferrite shows relatively broad, nearly rectangular hysteresis loops, as they are typical for easy-axis measurements, maghemite shows oppositely very small coercive fields and hysteresis loops similar to hard-axis measurements. Depending on the distances between the nanoparticles, the coercive fields vary in different ways, so that no common trend for both materials can be defined. Our results show that more investigations are necessary to fully understand nanoparticles distributed in polymeric or other nonmagnetic matrices, as they are used in diverse applications.

Data availability

Data will be made available on request.

Declaration of Competing Interest

The authors declare that they have no known competing financial interests or personal relationships that could have appeared to influence the work reported in this paper.

Acknowledgements

This research was partly funded by the German Federal Ministry for Economic Affairs and Energy (grant no. KK5129710KT1).

References

[1] R. Barbucci, D. Pasqui, G. Giani, M. De Cagna, M. Fini, R. Giardino, A. Atrei, A novel strategy for engineering hydrogels with ferromagnetic nanoparticles as crosslinkers of the polymer chains. Potential applications as a targeted drug delivery system, Soft Matter 7 (2011) 5558–5565.
[2] Y. Slimani, B. Unal, E. Hannachi, A. Selmi, M.A. Almessiere, M. Nawaz, A. Baykal, I. Ercan, M. Yildiz, Frequency and dc bias voltage dependent dielectric properties and electrical conductivity of $BaTiO_3SrTiO_3/(SiO_2)_x$ nanocomposites, Ceram. Int. 45 (9) (2019) 11989–12000.
[3] A. Saxena, S.S. Godara, Magnetic nano composite materials: A review, AIP Conf. Proc. 2148 (2019) 030022.
[4] A. Mamun, M. Klöcker, T. Blachowicz, L. Sabantina, Investigation of the Morphological Structure of Needle-Free Electrospun Magnetic Nanofiber Mats, Magnetochemistry 8 (2021) 25.
[5] G. Reiss, A. Hütten, Applications beyond data storage, Nat. Mater. 4 (10) (2005) 725–726.
[6] D. Vokoun, S. Samal, I. Stachiv, Magnetic Force Microscopy in Physics and Biomedical Applications, Magnetochemistry 8 (2022) 42.
[7] A. Remhof, A. Schumann, A. Westphalen, T. Last, U. Kunze, H. Zabel, Dipolar interactions in periodic arrays of rectangular ferromagnetic islands, J. Magn. Magn. Mater. 310 (2) (2007) e794–e796.
[8] J. Mejía-López, D. Altbir, A.H. Romero, X. Batlle, I.V. Roshchin, C.-P. Li, I.K. Schuller, Vortex state and effect of anisotropy in sub-100-nm magnetic nanodots, J. Appl. Phys. 100 (10) (2006) 104319.
[9] A. Ehrmann, T. Blachowicz, Vortex and double-vortex nucleation during magnetization reversal in Fe nanodots of different dimensions, J. Magn. Magn. Mater. 475 (2019) 727–733.
[10] J. Cheraghalizadeh, M.N. Najafi, Ising ferromagnets in Ising-percolation square lattices, an example of Ising-Ising coupling, Phys. Rev. E 98 (2018) 052136.
[11] M. Anand, Hysteresis in two dimensional arrays of magnetic nanoparticles, J. Magn. Magn. Mater. 540 (2021) 168461.
[12] X.u. Wang, D. Lv, L. Sun, W. Wang, X.-H. Tu, Z.-H. Ma, Magnetic behaviors of a ferrimagnetic decorated kagome-like lattice under an external magnetic field, J. Magn. Magn. Mater. 538 (2021) 168259.
[13] C.E. Ávila-Crisóstomo, E. Sánchez-Mora, V. Garcia-Vazquez, F. Pérez-Rodríguez, Magnetic response of Fe nanoparticles embedded in artificial SiO_2 opals, J. Magn. Magn. Mater. 465 (2018) 252–259.
[14] V. Russier, J.J. Alonso, I. Lisiecki, A.T. Ngo, C. Salzemann, S. Nakamae, C. Raepsaet, Phase diagram of a three-dimensional dipolar model on an fcc lattice, Phys. Rev. B 102 (2020) 174410.
[15] B. Zapotoczny, M.R. Dudek, N. Guskos, J.J. Koziol, B.V. Padlyak, M. Kosmider, E. Rysiakiewicz-Pasek, FMR study of the porous silicate glasses with Fe_3O_4 magnetic nanoparticles fillers, J. Nanomater. 2012 (2012) 341073.
[16] D.V. Perov, A.B. Rinkevich, Dynamic Permeability of Composite Media with Nonspherical Ferromagnetic Particles, Phys. Met. Metall. 123 (2) (2022) 138–144.
[17] N. Gack, G. Iankevich, C. Benel, R. Kruk, D. Wang, H. Hahn, T. Reisinger, Magnetotransport Properties of Ferromagnetic Nanoparticles in a Semiconductor Matrix Studied by Precise Size-Selective Cluster Ion Beam Deposition, Nanomaterials 10 (2020) 2192.
[18] N. Fokin, T. Grothe, A. Mamun, M. Trabelsi, M. Klöcker, L. Sabantina, C. Döpke, T. Blachowicz, A. Hütten, A. Ehrmann, Magnetic Properties of Electrospun Magnetic Nanofiber Mats after Stabilization and Carbonization, Materials 13 (2020) 1552.
[19] S. Layek, H.C. Verma, Room temperature ferromagnetism in Mn-doped NiO nanoparticles, J. Magn. Magn. Mater. 397 (2016) 73–78.
[20] M.-K. Kim, P. Dhak, H.-Y. Lee, J.-H. Lee, M.-W. Yoo, J. Lee, K. Jin, A. Chu, K.T. Nam, H.S. Park, S. Aizawa, T. Tanigaki, D. Shindo, M. Kim, S.-K. Kim, Self-assembled magnetic nanospheres with three-dimensional magnetic vortex, Appl. Phys. Lett. 105 (23) (2014) 232402.
[21] T. Schrefl, G. Hrkac, D. Suess, W. Scholz, J. Fidler, Coercivity and remanence in self-assembled FePt nanoparticle arrays, J. Appl. Phys. 93 (10) (2003) 7041–7043.
[22] M. Agrawal, B. Rana, A. Barman, Magnetization reversal in chains and clusters of exchange-coupled nickel nanoparticles, J. Phys. Chem. C 114 (25) (2010) 11115–11118.
[23] B. Rana, M. Agrawal, S. Pal, A. Barman, Magnetization reversal dynamics in clusters of single domain Ni nanoparticles, J. Appl. Phys. 107 (9) (2010) 09B513.
[24] J. Fidler, P. Speckmayer, T. Schrefl, D. Suess, Numerical micromagnetics of an assembly of (Fe, Co) Pt nanoparticles, J. Appl. Phys. 97 (10) (2005) 10E508.
[25] M. Wortmann, A.S. Layland, N. Frese, U. Kahmann, T. Grote, J.L. Storck, T. Blachowicz, J. Grzybowski, B. Hüsgen, A. Ehrmann, On the reliability of highly magnified micrographs for structural analysis in materials science, Sci. Rep. 10 (2020) 14708.
[26] T. Blachowicz, J. Grzybowski, A. Ehrmann, Micromagnetic simulations of nanoparticles with varying amount of agglomeration, Macromol. Symp. 402 (1) (2022) 2100381.
[27] T. Blachowicz, A. Ehrmann, Most recent developments in electrospun magnetic nanofibers: A review, J. Eng. Fibers Fabr. 15 (2020), 1558925019900843.
[28] N. Torasso, A. Vergara-Rubio, P. Rivas-Rojas, C. Huck-Iriart, A. Larrañaga, A. Fernández-Cirelli, S. Cerveny, S. Goyanes, Enhancing arsenic adsorption via excellent dispersion of iron oxide nanoparticles inside poly(vinyl alcohol) nanofibers, J. Environ. Chem. Eng. 9 (1) (2021) 104664.
[29] S.M. Hosseini, M. Abdouss, S. Mazinani, A. Soltanabadi, M. Kalaee, Modified nanofiber containing chitosan and graphene oxide-magnetite nanoparticles as effective materials for smart wound dressing, Comp. Part B Eng. 231 (2022) 109557.
[30] W. Scholz, J. Fidler, T. Schrefl, D. Suess, R. Dittrich, H. Forster, V. Tsiantos, Comput. Mater. Sci. 28 (2003) 366–383.
[31] D.V. Berkov, J. Miltat, Spin-torque driven magnetization dynamics: Micromagnetic modeling, J. Magn. Magn. Mater. 320 (2008) 1238–1259.
[32] M. Haidar, A.A. Awad, M. Dvornik, R. Khymyn, A. Houshang, J. Akerman, A single layer spin-orbit torque nano-oscillator, Nature Commun. 10 (2019) 2362.
[33] N.A. Usov, R.A. Rytov, V.A. Bautin, Properties of assembly of superparamagnetic nanoparticles in viscous liquid, Sci. Rep. 11 (2021) 6999.